Shake table testing of scaled geogrid-reinforced adobe wall models

J.F. Tipler[1], M.L. Worth[1], H.W. Morris & Q.T. Ma

Department of Civil Engineering, University of Auckland, Auckland.

2010 NZSEE Conference

ABSTRACT: Adobe is a weak, brittle earth building material. Unreinforced adobe walls are extremely vulnerable during seismic events. This paper presents the findings of an investigation into the dynamic performance of adobe walls reinforced with geogrid mesh. One-third scale models of adobe earth walls, loaded out-of-plane, performed well when subjected to 0.8g static tilt tests and uni-directional dynamic accelerations up to 1.07g at the University of Auckland. Two walls were built to comply with the requirements of *NZS 4299:1998 Earth Buildings Not Requiring Specific Design.* One wall was nominally reinforced with only vertical steel at the corners and one was fully reinforced with steel vertical reinforcement for high seismic hazard and polysynthetic geogrid horizontal reinforcement every third course in the mortar layer.

Scale dynamic testing demonstrated the contribution of the vertical reinforcement to the structural integrity of the unreinforced wall. The geogrid horizontal reinforcement, which is required for in-plane strength, contributed little to the out-of-plane performance until load levels were near maximum. The geogrid significantly improved potential life safety by reducing the size of falling debris and preventing wall collapse. The geogrid contributed to out-of-plane stiffness and integrity although full scale tests would be required to quantify these benefits.

1 INTRODUCTION

Sun-dried adobe bricks are one of the most widely used building materials in the world. However, adobe houses are very susceptible to sudden collapse during seismic loading, often resulting in great loss of life (Samali et al., 2008). This is partly due to the low ductility and tensile strength of adobe, (Tolles, 1989) and the large mass of adobe structures, which means that adobe attracts far greater seismic loads than other lightweight building materials (Charleson and French, 2005).

The typical failure mechanism of unreinforced adobe houses during seismic events involves vertical corner cracking at the intersection of orthogonal walls and mid-span vertical cracking in the out-of-plane wall (Samali et al., 2008). Reinforcement systems must aim to prevent this mode of failure, and other sudden failure mechanisms so occupants have time to evacuate the building before collapse.

Earthen construction has become increasingly popular in New Zealand since the 1980s, providing a sustainable alternative to traditional building practices. In 1998 a suite of three earthen construction standards was released to regulate the construction of earthen wall buildings in New Zealand (Morris, 2005). Around a dozen adobe houses are constructed annually in New Zealand, the only country where geogrid is used in the wall mortar layer.

This study focuses on *NZS4299: Earth Buildings Not Requiring Specific Design* (Standards NZ, 1998); in particular, focusing on the specification of geogrid as one of three possible horizontal reinforcement materials for adobe walls. The use of geogrid is intended to increase the seismic performance of the in-plane walls by restricting cracking caused by diagonal tension. The primary objectives of this research were to confirm that the use of geogrid provides adequate earthquake

[1] Final year undergraduate students

reinforcement when used in accordance with NZS4299 and does not reduce the out-of-plane wall performance by introducing horizontal planes of weakness.

2 CONSTRUCTION DETAILS OF ADOBE TEST WALLS

Two U-shaped adobe test walls were constructed at a scale of 1:3. The first represented a nominally reinforced wall, which had 4mm vertical steel bars at the intersection of orthogonal walls and a structural bond beam. The second represented a wall fully reinforced with additional vertical steel reinforcement for high seismic hazard, and polysynthetic geogrid, placed horizontally every third course in the mortar layer. The walls were 1.47m long, 0.8m high and were supported by 0.65m in-plane anchored return walls. The u-shaped arrangement of the wall allowed the connection and restraint of the in-plane shear walls to be effectively modelled, whilst keeping the overall weight of the model low, which was limited by the capacity of the shake table.

The two wing walls were tied down by additional steel rods and a wooden beam that simulated the restraint of continuous in-plane walls (Fig. 2.1). The wooden bond beam was 90mm x 22mm, anchored to both of the adobe models, in compliance with *NZS 4299: Earth Buildings Not Requiring Specific Design.*

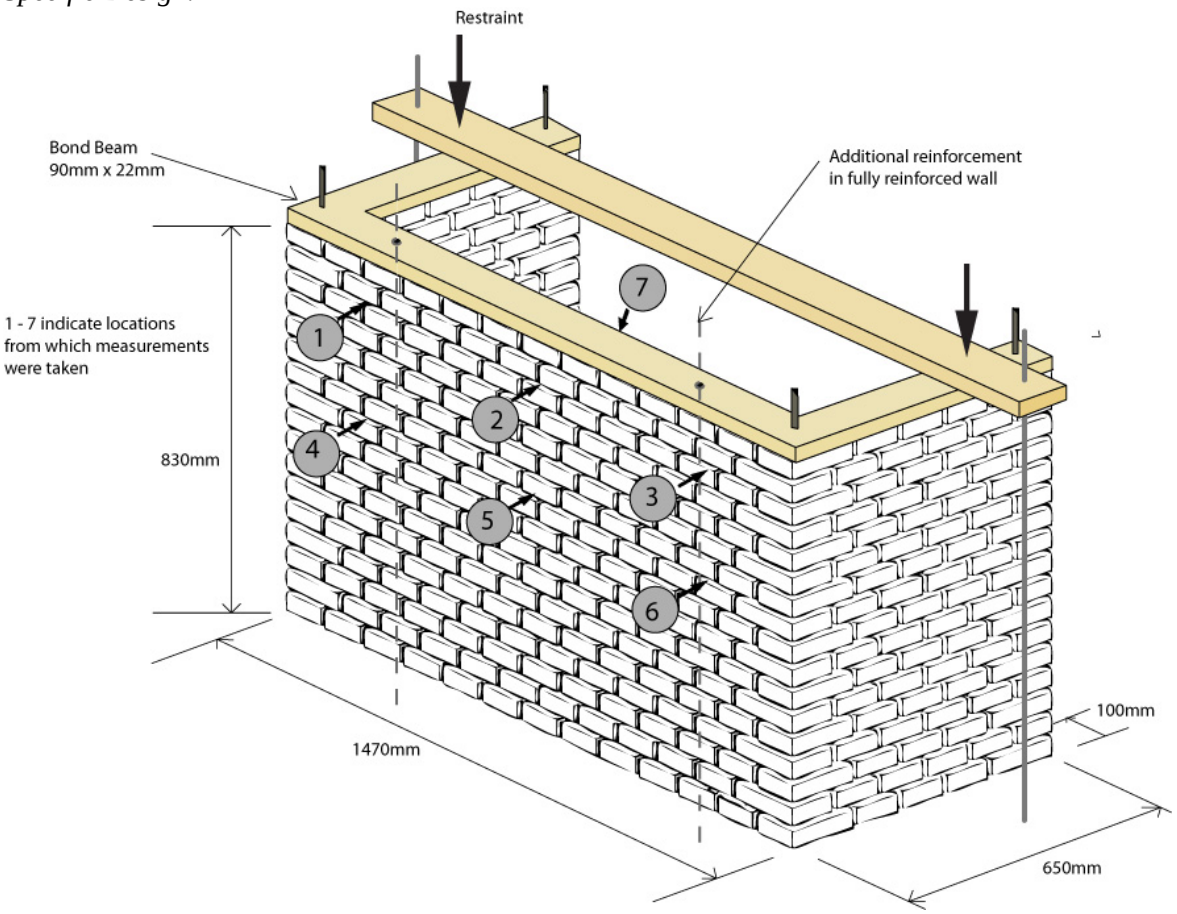

Figure 2.1 Set up of model U-shaped wall showing instrument locations

Small-scale Microgrid® was used in the fully-reinforced wall, in accordance with stiffness based scaling laws proposed by Iai (1989). The geogrid was laid horizontally between thin layers of mortar every third course, and was fastened to the vertical reinforcement at the corners.

3 DYNAMIC TESTING OF ADOBE WALLS

Each wall was initially subjected to a number of sine sweep waves, between 1 and 50 Hz, to gauge the pre-cracked dynamic behaviour of the wall. This was suceeded by three earthquake records that

differed in peak ground acceleration (PGA), frequency content and length. The records were run at the serviceability limit state (SLS) and finally at ultimate limit state (ULS). The El Centro record was chosen, as it is the most commonly tested record and allowed comparisons with other tests. The 1994 Northridge record was used because it has forward directivity and the 1985 Llolleo, Chile earthquake was used because of its relatively long duration. Earthquakes with these characteristics were deemed most likely cause collapse of the adobe walls.

The PGA of each earthquake was scaled according to the procedure set out in *NZS 1170.5 Structural Design Actions: Part 5 - Earthquake Actions* (Standards NZ, 2004). The parameters used to determine the earthquake record scaling were based on the worst-case scenario; the scaling factors are summarized in Table 3.1.

Table 3.1 Earthquake Scaling Factors

Earthquake Record	k(SLS)	k(ULS)
El Centro, California, 1940	0.1242	0.3549
Northridge, California, 1994	0.4648	1.3279
Llolleo, Chile, 1985	0.5675	1.6213

The geogrid reinforced wall did not collapse during shake table testing using inputs from earthquake records, and was consequently subjected to additional sine sweep waves, with the intention of damaging the wall; these have been summarised in Table 3.2.

Table 3.2 Sequence of Additional Destructive Sine Sweep Waves Tests Undertaken on Geogrid-Reinforced Wall

Order	Test Description *	Order	Test Description *
a	10 Hz 30s 1.05g	e	12 Hz 0.8g
b	12 Hz 20s 1.5g	f	12 Hz 1.6g
c	2-16 Hz 0.2g	g	14 Hz 1g
d	4-16 Hz 0.28g	h	Manual sine

* The above table specifies intended shake table accelerations; these did not always correspond to actual table acceleration, due to limitations in the capacity of the shake table.

3.1 **Description of Equipment**

3.1.1 *Instrumentation*

Three linear variable differential transducers (LVDTs) and three portal gauges were used to measure relative wall displacement. An accelerometer was also used to measure the acceleration of the wall. Additionally, the acceleration, velocity and displacement of the shake table were recorded.

During testing of the partially reinforced wall, the LVDTs were placed in locations 1-3 (see Fig. 2.1) and the strain gauges were in 4-6. The mid-span accelerometer located at number 7, and LVDT located at number 2, did not record useful data during the first test of the nominally reinforced wall. Therefore, accelerations and displacements used for comparative purposes have been gauged from LVDT 5. During the first test it was observed that maximum displacements were occurring closer to mid height rather than at the top of the wall. For testing of the fully reinforced wall, the position of the LVDTs and strain gauges were swapped as a result.

3.1.2 *Shake Table Specifications*

University of Auckland small shake table specifications

Size of table	1m x 1.5m
Maximum payload	1 tonne
Payload from one specimen	<600 kg

Maximum displacement	100 mm
Maximum Velocity (600kg)	0.69 m s^{-1}
Maximum Acceleration (600 kg)	16.5 m s^{-2}
Testing Frequency	1-50 Hz

4 STATIC TESTING OF ADOBE WALLS

A static tilt test was performed in order to gain comparative displacement data from both walls under a known acceleration. The wall was tilted so that it experienced gravitational accelerations; the resultant displacements were read at mid height of the wall using displacement gauges and the gravitational accelerations experienced by the wall were calculated from the angle. Both walls were tilted from five degrees to fifty degrees in five degree increments. The wall was tilted using the gantry crane to lift one side of the base plate. An angle section was bolted to the floor to prevent sliding of the base plate. This test was performed following the dynamic testing, using the same models.

Figure 4.1 Tilt Test in Progress

5 RESULTS AND DISCUSSION

5.1 Dynamic Testing

As both models had approximately the same fundamental frequency of 12Hz, it can be assumed that the stiffness of the models was similar. Dispacement is a function of stiffness and mass, so this indicates that the pre-cracked walls were expected to have similar displacements, under identical earthquake forces. The position of maximum deflection in both the pre-cracked walls was observed to be mid wall around ¾ height. This observation was used with the displacement profiles to create approximation of the pre-crack deflections as shown in Figure 5.1.

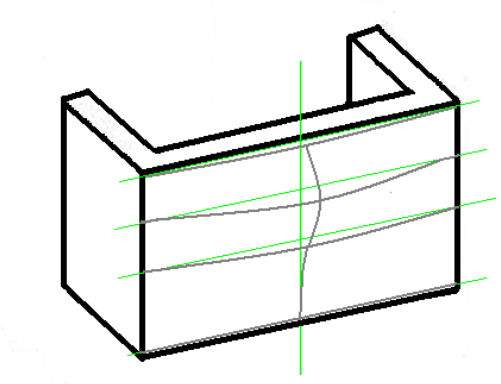

Figure 5.1 Approximated deflected shape of the pre cracked walls

5.1.1 *Initial Cracking*

Similar patterns of initial cracking were observed in both walls, but it was apparent that the geogrid prevented signifigant initial cracking. The partially reinforced wall first cracked during the Llolleo Ultimate Limit State (ULS) earthquake. For the fully reinforced wall no cracks were visible after it was subjected to the similar Llolleo ULS earthquake. The capacity of the table meant that adequately high level earthquake records could be applied, and the first significant cracks formed in the fully reinforced wall during a 10 Hz destructive sine sweep at 1.05g. In both walls, the first crack to form was a horizontal crack in the mortar below the top layer of bricks. High shear stresses acted in this layer because the top brick layer was fixed to the bond beam. The crack propagated along the entire mortar layer in the partially reinforced wall. However it was significantly shorter in the fully reinforced wall, indicating that the additional reinforcing provided tensile strength across the crack and reduced the crack's propagation. Horizontal cracks also formed in the top half of the wall around the position of maximum deflection, and were likely to have formed from high flexural stresses in the vertical span. The vertical span was shorter and hence had greater curvature and increased flexural stresses. Cracks in the horizontal plane therefore occurred before vertical cracking.

5.1.2 *Post-Cracked Behaviour*

After initial cracking, the vertical span no longer had significant lateral restraint at the top of the wall and deflected more like a cantilever. This transferred greater flexural stresses to the horizontal span. This resulted in a deflected shape for both walls as shown in the conceptual diagram (Fig. 5.4).

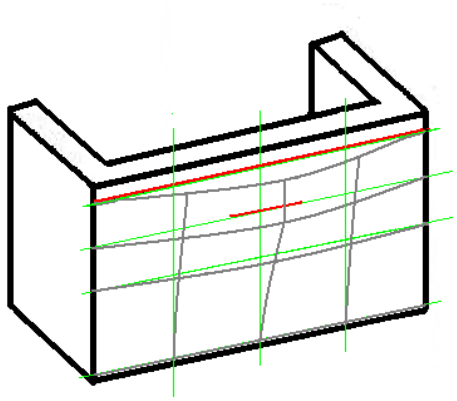

Figure 5.4 Exaggerated deflections of walls after initial cracking

In the partially reinforced wall a large vertical crack formed at mid-span due to flexural stresses in the horizontal span, which propagated into a diagonal crack (Fig. 5.5).

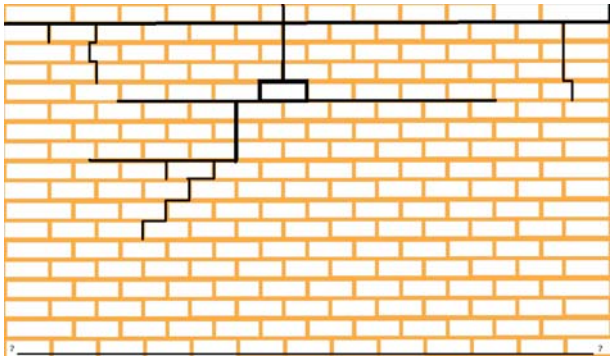

Figure 5.5 Cracking just before collapse of Partially Reinforced wall (Llolleo earthquake record (4xULS) at 27seconds)

The large horizontal and vertical cracks effectively caused two horizontal 'cantilevers' to form at the top of the wall. The response of the cantilevers to the earthquake motion caused large flexural cracks at the intersection of the out-of-plane wall and the perpendicular wing walls. (Fig. 5.6).

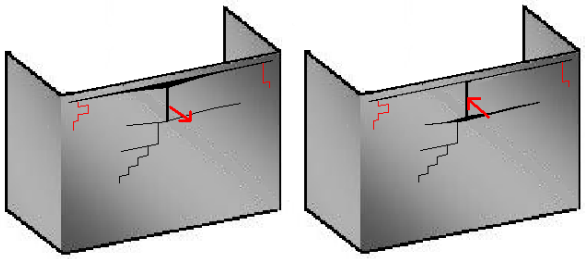

Figure 5.6 Splitting crushing cycle at wall intersection.

In the fully reinforced wall, small and closely spaced vertical flexural cracks formed, due the geogrid causing a more even distribution of flexural stresses and reduced the horizontal “cantilever” effect (Figs. 5.6, 5.7).

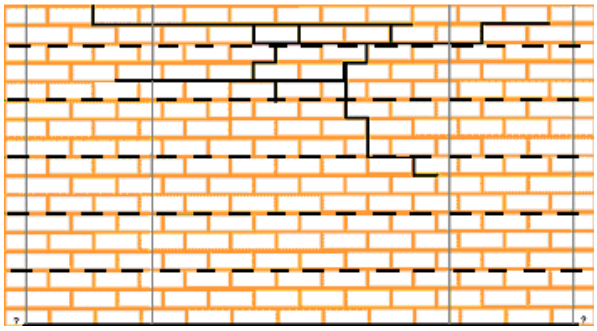

Figure 5.7 Cracking just before collapse of Fully Reinforced wall (12 Hz destructive sine sweep (1.5g) at 3 seconds)

In Figure 5.7 the dashed horizontal lines indicate the position of the geogrid on the wall. No tendency for cracks to propagate in the geogrid layer was observed, so the geogrid was not creating a plane of weakness.

5.1.3 *Collapse Sequence*

The partially reinforced wall collapsed 28 seconds into the Llolleo earthquake record, which was at four times the ultimate limit state.

Table 5.1 Collapse sequence of partially reinforced wall

Crack Pattern	Time	Crack Pattern	Time
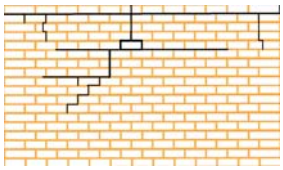	Llolleo earthquakerecord (4xULS) at27seconds	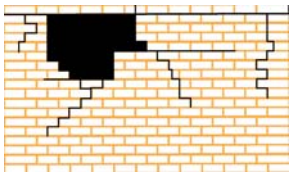	Llolleo earthquake record (4xULS) at 38seconds
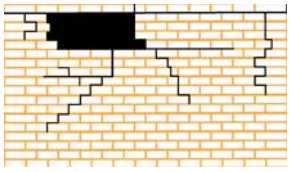	Llolleo earthquakerecord (4xULS) at30seconds		

The large and widely spaced cracking caused the wall to fall out in a two large blocks. The largest block consisted of sixteen bricks. The accelerometer mount near the centre appears to have prevented the right hand side of the wall from falling.

***Table 5.2* Collapse sequence of fully reinforced wall**

Crack Pattern	Time	Crack Pattern	Time
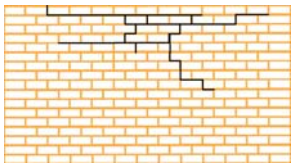	12 Hz destructive sine sweep (1.5g) at 3 seconds	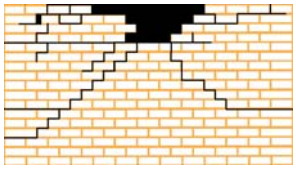	4-16Hz destructive sine sweep (0.28g) at 2minutes 25 seconds
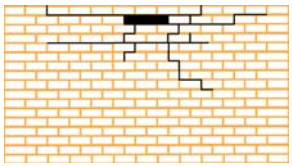	12 Hz destructive sine sweep (1.5g) at 4 seconds	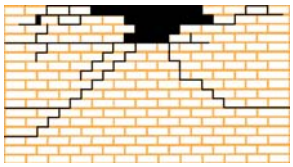	Manual destructive sine sweep at 1minute 47 seconds
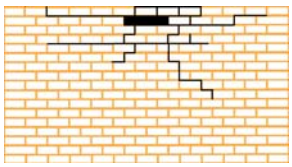	12 Hz destructive sine sweep (1.5g) at 7 seconds	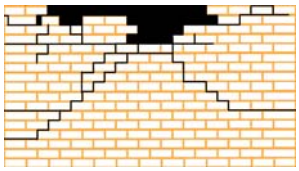	Manual destructive sine sweep at 1minute 50 seconds
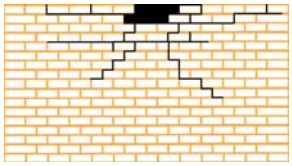	12 Hz destructive sine sweep (1.5g) at 9 seconds	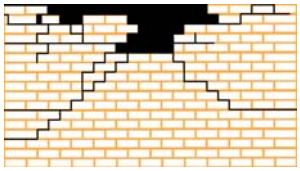	Manual destructive sine sweep at 1minute 55 seconds
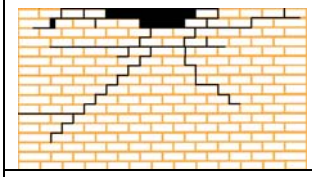	12 Hz destructive sine sweep (1.5g) at 17 seconds	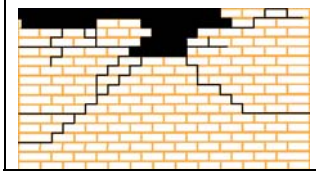	Manual destructive sine sweep at 2 minutes
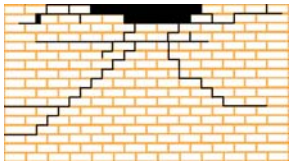	4-16 Hz destructive sine sweep (0.28g) at 2 minutes 11 seconds		

In both walls cracking occurred through the bricks as well as the mortar. In a full-scaled wall we would have expected cracking to run mainly through the mortar layer. This scale effect is due to the smaller bricks having a greater surface area to volume ratio than larger bricks. The larger surface area creates a better proportionate mortar bond and the tendency for the walls to act monolithically.

5.1.4 *Final Crack Pattern of the Fully Reinforced Wall*

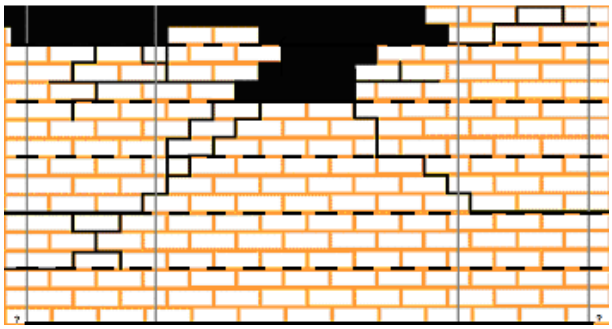

Figure 5.8 Final crack pattern of fully reinforced wall

Figure 5.8 shows the final crack pattern in relation to the position of the geogrid, which is indicated by the dashed horizontal lines. At the base of the wall cracks tended to form in the geogrid layer but no sliding was observed, indicating that a plane of weakness had not formed. The photograph (Fig. 5.9). shows a crack that progressed through the geogrid layer and then passed through the top of the mortar layer and not along the plane of the geogrid .

Figure 5.9 Crack running through geogrid layer on bottom right hand side of wall.

5.1.5 *Cracking in the Wing Walls*

In both models, vertical tensile cracking of the orthogonal wing walls was observed at the intersection between these walls and the out of-plane-wall (Fig. 5.10). These cracks formed as the out-of-plane wall began to collapse. From the video footage, it was difficult to determine whether the geogrid had any effect on the propagation of cracks occurring in the out-of-plane wall

a) **b)**

Figure 5.10 Vertical tensile cracks in the a) partially reinforced wing wall, and b) fully reinforced wing wall

5.2 **Static testing**

The results from the tilt test enabled a comparison between the magnitudes of displacement occurring when both models were subject to the same equivalent acceleration. The tilt test used the damaged adobe models so the results are only relevant to post-cracked behaviour of the walls. The fully reinforced wall had smaller deformations than the partially reinforced model demonstrating that the geogrid provides additional stiffness to the post- cracked adobe wall (Fig. 5.11).

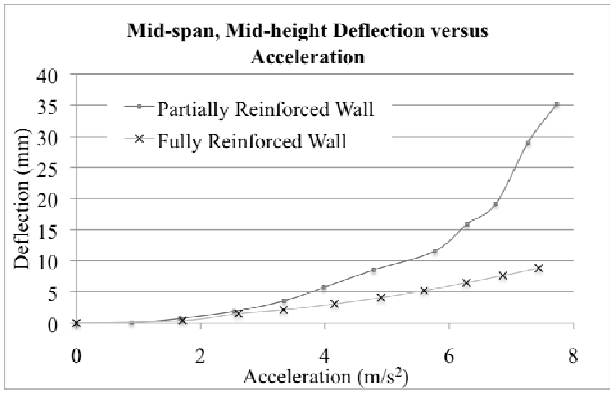

Figure 5.11 Graph of wall deflection versus acceleration during static testing of the adobe walls.

6 **DISCUSSION**

6.1 **Dynamic response**

Both of the model walls withstood substantial earthquake forces, indicating better seismic performance than expected. The partially reinforced wall was able to endure twice the Llolleo scaled ultimate limit state motion; with the upper wall section collapsing at four times the ULS. The fully-reinforced model performed better and a brick by brick collapse of the upper wall was produced by applying a sustained destructive sine sweep at its resonant frequency of 12Hz. This enhanced seismic performance was partly due to scaling effects; this is evident in the cracks propagating through the bricks as well as the mortar, indicative of monolithic behaviour.

Quantitative analysis of pre-cracked behaviour gives some indication of the mode shape of the adobe walls (Fig 3.1). Instrumentation failures and shake table limitations did not permit detailed comparison of dynamic deflections. Thus, there is no evidence that geogrid reinforcement improved the stiffness of the pre-cracked adobe walls, but there is evidence that addition of geogrid delayed initial cracking.

6.2 **Qualitative evaluation**

The qualitative analysis showed that geogrid reinforcement improved the collapse resistance of the adobe walls. The failure mechanism in both walls resulted from a combination of horizontal and vertical flexural cracking. The geogrid reinforcement distributed flexural stresses within the horizontal span of the wall, creating smaller and more closely spaced vertical cracks compared to the partially reinforced model, depicted in tables 5.1 and 5.2. This caused collapse to occur in smaller blocks in the fully reinforced wall, with the largest falling piece consisting of three bricks. Conversely, the largest block to collapse from the partially-reinforced wall consisted of 16 bricks. The fully reinforced wall small block failure mechanism also prevented large cracks from forming at the intersection of orthogonal walls. The corner failure is common in unreinforced out-of-plane walls and often leads to wall overturning and roof collapse. Geogrid reinforcement would significantly reduce the risk of injury to the occupants of a full-scaled house during a major seismic event.

Both walls performed well in the static tests with the partially reinforced wall maintaining unexpected integrity largely due to the vertical reinforcement continuous from the base to the bond beam.

6.3 **Geogrid effects**

There was no evidence of a strong tendency for cracks to form in the geogrid layers; and no sliding was observed when cracks did propagate through the geogrid layer. These results refute the concern of planes of weakness forming due to geogrid in the out-of-plane adobe wall. Bond-wrench testing demonstrated that the mortar layer containing geogrid had significantly higher flexural bond strength than the ordinary mortar layers.

6.4 **Limitations**

There are limits to the conclusiveness of this research with the primary limitation being the size and capacity of the University of Auckland shake table. The weight of the wall specimens meant it was not viable to carry out a truly comparative testing regime, as the shake table could not provide the walls with accelerations and displacements that were great enough to cause complete collapse using earthquake records alone. The fully reinforced wall was instead subjected to a number of additional sine sweeps so that the failure mechanism of this wall could be estimated.

Further research is needed to confirm that the results of this research are typical. It is also desirable to perform several repetitions of the test, and perform comparative tests on the two other horizontal reinforcement materials specified by NZS 4299. Future studies should also consider the effects of roof weights, wall thickness, spacing of vertical reinforcement and performing tests on scaled geogrid.

7 **CONCLUSIONS**

The use of geogrid as a horizontal reinforcment reduced the severity of collapse in the fully reinforced wall. This would significantly reduce the risk of injury to the occupants of a full-scaled house during a severe seismic event.

This study refutes that the concern of planes of weakness forming through the inclusion of geogrid in the out-of-plane adobe wall.

Concerns about the validity of the assumptions made in NZS: 4299 have largely been alleviated, although further testing is needed to confirm our preliminary conclusions.

Further testing should include repetition of our tests, or full-scale testing of geogrid-reinforced walls, using full-scale geogrid.

AKNOWLEDGEMENTS

The authors would like to thank technicians Tony Daligan, Mark Byrami and Sujith Padiyara for their support and express gratitude to Graeme North for his enthusiasm and expertise pertaining to adobe construction.

REFERENCES

Charleston, A. & French, M. 2005. Improving seismic safety of adobe construction with used car-tyre strips: preliminary investigations. *NZ Society for Earthquake Engineering Conference 2005, Paper 32*

Iai, S. 1989. Similatude for shaking table tests on soil-structure-fluid model on 1g gravitational field. *Soils and Foundations,* 29(1), 105-118.

Samali, B., Dowling, D. & Li, J. 2008. Dynamic testing and analysis of adobe-mudbrick structures. *Australian Journal of Structural Engineering,* 8**,** 63-75

Standards NZ, 1998. NZS 4299:1998 Earth Buildings Not Requiring Specific Design. Standards New Zealand, Wellington.

Standards NZ, 2004. NZS1170.5. Structural Design Actions Part 5 Earthquake Actions - New Zealand. Standards New Zealand, Wellington.

Tolles, L. 1989. Seismic Studies on Small-Scale Models of Adobe Houses. *Department of Civil Engineering.* PhD Dissertation, Stanford University.